Sustainable Energy, 2019, Vol. 7, No. 1, 6-14
Available online at http://pubs.sciepub.com/rse/7/1/2
Published by Science and Education Publishing
DOI:10.12691/rse-7-1-2

The Utilization of Renewable Energy Source and Environment Friendly Refrigerants in Cooling Mode

Ali H. Tarrad*

Mechanical Engineering, Consultant Engineer/Thermal Engineering Specialist, France
*Corresponding author: dr.alitarrad@gmail.com

Received August 08, 2019; Revised September 15, 2019; Accepted September 20, 2019

Abstract This investigation focuses on the renewable geothermal energy source utilized as a reservoir for a water chiller unit in the cooling mode. Two hydrocarbon refrigerants, R290 and R600a were suggested to be implemented in a closed loop system to produce chilled water for air conditioning purposes. The traditional R-22 and its substitute R410A were also investigated in a direct expansion geothermal system. The analysis was carried out at the evaporation and condensation temperature ranges of (-25 to -5) °C and (15 to 35) °C respectively. The data showed that R-290 revealed similar coefficient of performance as that of R-22. R-410A exhibited a lower coefficient of performance than that of the R-22 refrigerant by (1-5) %. On the contrary, R-600a showed a higher coefficient of performance than that of the R-22 by about (3) % for the investigation range of operating conditions. R-410A refrigerant exhibited the highest load in comparison with R-22 among other circulated refrigerants by (1.5) %. R-600a showed a lower condenser load than that of the R-22 system by a negligible margin value. The hydrocarbon refrigerants and the azeotrop mixture were found to be proper candidates to replace R-22 in geothermal system.

Keywords: *geothermal energy source, refrigerant alternatives, hydrocarbon refrigerants, water chillers*

Cite This Article: Ali H. Tarrad, "The Utilization of Renewable Energy Source and Environment Friendly Refrigerants in Cooling Mode." *Sustainable Energy*, vol. 7, no. 1 (2019): 6-14. doi: 10.12691/rse-7-1-2.

1. Introduction

The awareness and concerns towards the environment pollution, Ozone layer depletion and warming potential of earth occupied a great deal of attention by the international community for few decades ago. The natural available heat sources had attracted the scientists to implement such sources for the modern life technology and to invent a variety of technical philosophy for their usage. This was due to the fact that these sources are clean, cheap and renewable. The other important issue for the sustainability of life on earth is the Ozone layer and its deterioration. The latter measure has forced the international community to seek refrigerant alternatives for the halocarbon ones to minimize their impact on the Ozone issue.

A numerous work has been conducted on the utilization of a renewable low temperature heat source by the implementation of cascade heat pump. The latter is implemented to raise the energy from the low level to the high level for heating and vice versa for cooling purposes. Reference [1] studied experimentally the performance of air to water heat pump, which circulates R134a and R410A as refrigerants on the high and low cycle respectively. They concluded that the performances are deteriorated at high water inlet temperature and low ambient temperature. The optimal intermediate temperature is increased as ambient temperature increases and water inlet temperature increases. Reference [2] investigated experimentally R410A/ R134a cascade cycle for variable refrigerant flow heat pump systems. The higher COP condition was obtained when the intermediate temperature was in the range (40-41) °C and the ambient temperature at 7°C regardless of the water inlet temperature to the high temperature condenser.

References [3-8] investigated the performance of cascade heat pump circulating pairs of environment friendly refrigerants when extracting the energy from seawater at low temperature for heating purposes. He studied a variety of issues in regards of the implementation of those systems such as evaporator temperature, intermediate temperature of cascade heat exchange, condensing temperature, CO_2 emission and the economic feasibility of such energy sources. Tarrad has stated that the implementation of seawater energy was more beneficial than that of natural gas firing, economically and environmentally [8].

Although the underground temperature is almost stable over the year round but it is a dependent measure on the altitude. The temperature in the ground below (6) m is roughly equal to the mean annular air temperature at that altitude. It is at the range of (10-16) °C. Seasonal variation decreases with depth and disappears below (7 to 12) m. This temperature behavior of the underground has attracted the scientists to the exploitation of ground as a heat source or a reservoir for heat rejection in the heating and cooling modes respectively. These goals were achieved by the utilization of heat pump technology. The coefficient of performance of this type of heat pumps is

ranged between (3) and (5) depending on the operating conditions, [9].

Reference [10] studied a ground source heat pump system performance with R407C/R134a. They postulated that the optimum condensing temperature of the low temperature side of the cascade heat pump lies in the (35-37) °C range. This was the case when the evaporating temperature of R407C at the low temperature evaporator and condensing temperature of R134a at the high temperature side are at (−5) °C and (65) °C respectively. Reference [11] concluded that when the flow rate was doubled from (1) l/min to (2) l/min in a ground heat source system, the average heat transfer rate was enhanced by about (21.7%) for standing ground heat exchanger (GHE) and (17.5%) for reclined (GHE). They also indicated that the seasonal change of the surrounding ground temperature of GHE has a significant effect on the overall performance of GHE.

A compound Cascade system was developed where three cycles in three pressure and temperature levels were integrated with two low temperature heat sources, underground and seawater [4]. In this study, R717/R134a system exhibited heating COP increase of about (3 %) higher than that of R410A/R134a system for both tested intermediate temperatures of (33 and 35) °C and condensing temperature of (70)°C. In addition, the specific power consumed by compressors of the proposed system arrangement showed a decrease of up to (3 %) lower than that of the seawater single source Cascade system operating under the same conditions.

In the present work, the thermal performance of a refrigeration system coupled with a renewable energy reservoir utilized in the cooling mode was investigated. A hypothetical system is to be implemented in a public or industrial zone where the cooling demand estimated to be (10) ton of refrigeration. The heat is withdrawn from the occupied zone and rejected to the reservoir assigned as the underground zone through a standard refrigeration unit. A direct exchange expansion or indirect geothermal systems which circulate hydrocarbon refrigerants such as R-290 or R-600a were utilized. R-410A was also studied as non-hydrocarbon azeotrop mixture refrigerant. A comparison of the thermal performance with that of the traditional R-22 unit was made at a temperature range of (-25) °C to (-5) °C.

2. Investigation Methodology

The harness of geothermal sustainable energy and environmental friendly refrigerants has been considered for many decades. It is inevitable that this source will be one of the most important energy sources in the global. It took a great consideration in the research and development with enormous effort to implement this concept in the domestic and industrial fields.

2.1. Refrigerants

The selected refrigerants for this study are presented in Table 1. These refrigerants represent three different physical categories of operating conditions.

- Nonflammable pure refrigerant assigned as R-22.
- Nonflammable azeotropic refrigerant mixture R-410A with a negligible temperature glide and high working pressure.
- Flammable pure hydrocarbon refrigerants assigned as R-290 similar working pressure as that of R-22 and R-600a as a low working pressure refrigerant.

Table 1. Physical and operating conditions of refrigerants

Property	R-22	R-410A	R290	R600a
Composition and Refrigerant (Formula)	CHCIF2 (100)%	R32/125 (50/50) % by Weight	C3H8 (100) %	C4H10 (100) %
Molecular Weight (kg/kmol)	86.47	72.58	44.1	58.12
Normal Boiling Point (°C)	-40.81	-51.58	-42.09	-11.7
Temperature Glide (°C)	0	< 0.2	0	0
Critical Pressure (MPa)	4.990	4.926	4.25	3.64
Critical Temperature (°C)	96.15	72.13	96.70	135
Ozone Depletion Potential	0.05	0	0	0
Global Warming Potential	1760	2088	3.3	3
Flammability and Toxicity*	A1	A1	A3	A3

* ASHRAE Safety Group 34: A1 – Non Flammable and A3 – Flammable, [12]

Such a variety of circulating refrigerants properties provides a perspective view for the aims of this study for the implementation of environment friendly refrigerants in a geothermal system. In addition, R-410A is also representing a high pressure refrigerant used widely at the present time in air conditioning systems. The flammable hydrocarbon refrigerants are also utilized in the available market units for heating and cooling purposes with a firm guide of safety regulations. These units cover refrigerators, water chillers, heat pumps and other modern applications.

The yard line is subject to depth requirements for the protection of the line and connections on either end of the system. Depths for service lines range from (12) to (18) inches underground is recommended for buried gas copper pipes, [13]. Hence, it is suggested to use the available standard regulation for the piping system when circulating the flammable hydrocarbon refrigerants R-290 and R-600a for the purpose of the present work. The firing properties of the hydrocarbon refrigerants R-290 and R-600a are compared to those of natural gas in Table 2.

Table 2. Comparison of firing properties of hydrocarbon refrigerants with natural gas

Property	R-290	R-600a	N. Gas
Flammability and Toxicity*	A3	A3	A3
Lower Flammability Limit (LFL)**: By Volume (%)	2.1	1.8	4.4
Upper Flammability Limit (UFL)**: By Volume (%)	9.5-10.1 [16]	9.6	15-16.4
Auto-ignition temperature (°C)**	470	460	580
Stoichiometric Combustion air/fuel ratio (kg. air/kg. fuel)	15.7	15	17.1

* ASHRAE Safety Group 34: A1 – Non Flammable and A3 – Flammable, [12]

** The practical limit as used in EN378 is defined as 20% of the LFL, [14,15].

These hydrocarbons share the same level of flammability and toxicity; hence the same safety regulations category could be implemented for test refrigerants.

The test refrigerants were not meant to replace R-22 in a drop-in technique. A new design is to be established for the refrigeration unit when circulating R-410A due to tis high working pressure, Figure 1. The other candidates probably need a soft modification for the existed refrigeration unit circulating R-22. The substitute R-600a possesses the lowest working pressure among other refrigerants whereas R-290 and R-22 have similar working pressure.

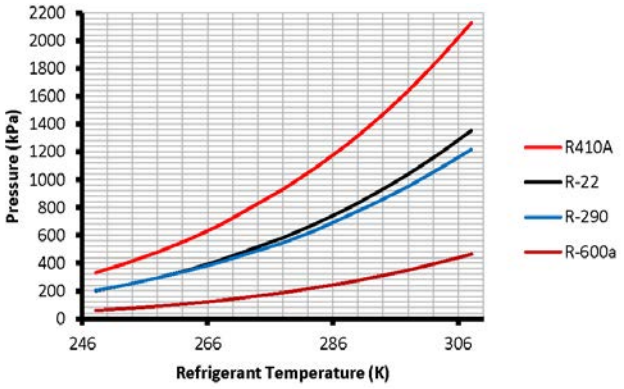

Figure 1. Saturation pressure versus temperature for test refrigerants

2.2. Refrigeration Unit

In this study, it is suggested to utilize the hydrocarbon refrigerants in a direct exchange (DX) geothermal system for cooling purposes, Figure 2. Such system requires more refrigerant amount than the usual air source units due to the copper tubing system involved for the condenser buried in the ground. It is a closed-loop, refrigerant-based geothermal system.

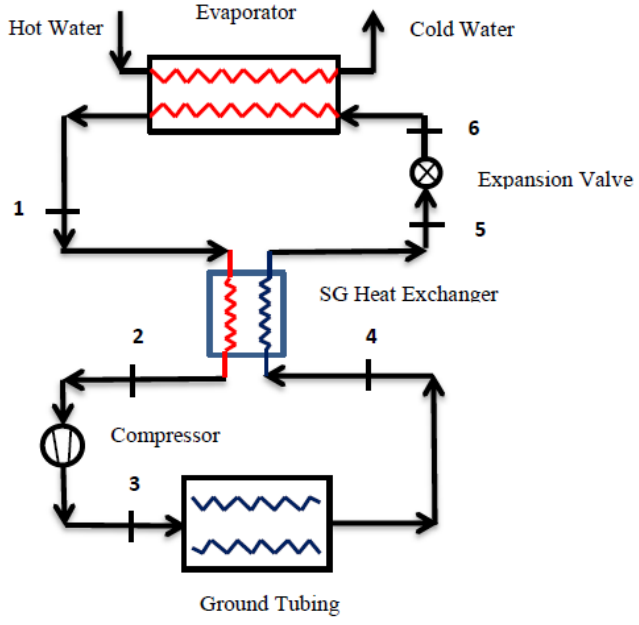

Figure 2. A schematic diagram for the geothermal direct energy exchange system

It has been found that the direct expansion system is more efficient than that of the indirect system where brine (water/propylene glycol) cycle to be introduced to the simple (DX) unit. This postulates that the ground loop in the (DX) unit is fabricated without the use of any intermediary for energy transfer process. This simplifies the fabrication of the system and raises its potential to reach high efficiencies with a reduced installation cost [17].

The (p-h) diagram of the hypothetical system layout is shown in Figure 3. The ports designations represent the actual flow direction of the refrigerant that is circulating through the water chiller as illustrated in Figure 2. The higher pressure zone of this system is laid between ports (3) and (5), at the discharge side out of the compressor and inlet port of the expansion device port respectively. It represents the refrigerant flow through the condenser and the suction gas heat exchanger for the liquid phase side. The zone bounded by the refrigerant path between ports (6) and (2) represents the lower operating pressure; it corresponds to the flow throughout the evaporator and suction gas heat exchanger in the vapor phase.

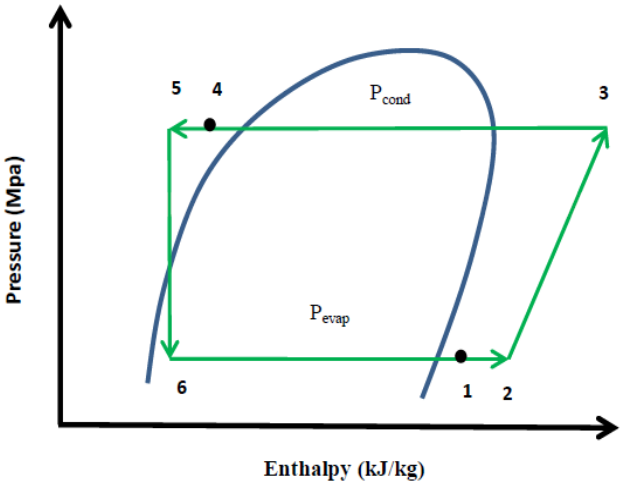

Figure 3. A schematic (p-h) diagram for the hypothetical water chiller

2.3. Operating Conditions

The following operating conditions of the cooling unit were implemented for all of the test refrigerants:

- A useful superheat degree in evaporators of (3) °C and subcool degree of (2) °C in condensers were assumed. Unuseful superheat in piping at the suction line was assumed to be (1) °C.
- A suction gas heat exchanger was assumed with a thermal efficiency of (30) % to subcool the condensed refrigerant and heat up the gas at the compressor suction line. This is to allow for energy recovery through the suction gas heat exchanger during water chiller operation for design purposes.
- Evaporation temperature was ranged between (-25) °C and (-5) °C at a step of (5) °C for all of the test refrigerants.
- Condensing temperature was ranged between (15) °C and (35) °C. The minimum temperature was selected to cover wider altitude and environment conditions in regard of the ground temperature.

- The compressors are operating at (70 %) and (80 %) isentropic and volumetric efficiencies respectively with (10 %) heat loss.
- Cooling load of (10) tons of refrigeration is to be extracted from the space throughout the circulation of chilled water in fan coils installed at the required points.
- Chilled water is to be produced by circulating through the chiller at temperature range of (7-12) °C.
- Rejected load to the ground by the copper tubing of the condenser was in the range of (40-50) kW.

2.4. Data Analysis

The data analysis utilizes the general energy criteria deduced from the first law of thermodynamics for evaporator, condenser, expansion valve and compressor. The energy loss from the evaporator was assumed to be negligible for excellent thermal insulation. Isentropic compression process at efficiency of (70) % and (80) % volumetric efficiency with allowance of (10) % heat loss for compressor was assumed. Hence the controlling equations for the thermal performance of the chiller were obtained. The designation of ports are used the same as those shown in Figure 2. The available code known as (CoolPack) was implemented wherever it was needed to collect the physical properties of the analyzed refrigerants and assessment verification objectives [18].

2.4.1. Evaporator

The energy balance in the evaporator gives the mass flow rate of refrigerant circulated through the heat exchanger as:

$$\dot{m}_{ref} = \frac{\dot{Q}_{evap}}{(h_1 - h_6)}. \quad (1)$$

2.4.2. Condenser

The refrigerant enters the condenser as superheated gas; the superheat value depends on the refrigerant type and operating conditions. Thermodynamics yields the following relation:

$$\dot{Q}_{cond} = \dot{m}_{ref}(h_3 - h_4). \quad (2)$$

2.4.3. Suction Gas Heat Exchanger

This equipment is used to capture heat from the condensed refrigerant and raise the suction gas temperature at the inlet port of compressor. Energy balance across this heat exchanger is used to calculate the suction enthalpy and hence the temperature of the gas at that port in the form:

$$\dot{m}_{ref}(h_4 - h_5) = \dot{m}_{ref}(h_2 - h_1). \quad (3)$$

In this relation the term $\dot{m}_{ref}$ is omitted from both sides since the same amount of refrigerant flow rate is passing through the heat exchanger.

2.4.4. Compressor Power Consumption

The power consumed by the proposed system depends mainly on the efficiency of the available compressor and technology. The ideal power consumed by the compressor to conduct a specific pressure lift is usually lower than that consumed during real operation of the compressor. The measure which reflects the amount of power to be spent is assigned as isentropic efficiency (η_{is}). The commercially available compressors have an isentropic efficiency laid in the range of (70 %) to (90 %). Hence, it was decided to select the minimum published isentropic efficiency of commercial compressors. Any increase in this factor will of course enhance the (*COP*) of the system considerably. The consumed power for compressor at a steady state flow can be estimated from:

$$\dot{W}_{comp} = \dot{m}_{ref}(h_3 - h_2) = \frac{\dot{m}_{ref}(h_{is} - h_2)}{\eta_{is}}. \quad (4)$$

Thus the actual amount of refrigerant sucked by the cylinder of the compressor for a reciprocating compressor is less than the amount of gas that it could have sucked theoretically based on the diameter of the bore and its length. The volumetric efficiency (η_{vol}) of the compressor is represented by the ratio of the actual sucked volume of gas to the theoretical volume that it could have sucked at the absence of the clearance volume. The clearance volume limits the stroke of the piston; hence it reduces the capacity of the compressor as well as its volumetric efficiency.

2.4.5. Coefficient of Performance (COP)

It represents the ability of the air conditioning apparatus to move heat from the air conditioned space to the underground reservoir throughout the copper tubing. Hence, the ability of the air conditioning unit to remove heat from the interior is expressed in terms of the cooling load as follows:

$$COP_{System} = \frac{\dot{Q}_{evap}}{\dot{W}_{comp}}. \quad (5)$$

2.4.6. Deviation Estimation (ψ)

The deviation of any predicted parameter as compared to that of R-22 values is estimated from:

$$\psi = \frac{(\phi_{ref} - \phi_{R-22})}{\phi_{R-22}} \times 100. \quad (6)$$

Here (ψ) represents the deviation percentage as compared to that of R-22 parameter. The variable parameter (ϕ) corresponds to any of the performance measures, power consumption ($\dot{W}_{comp}$), condenser load ($\dot{Q}_{cond}$) or coefficient of performance (COP_{System}).

3. Results and Discussion

3.1. Reference Refrigerant

The reference refrigerant used for performance comparison is the R-22 system. Figure 4 illustrates the consumed power variation with the evaporator temperature at different condensing temperatures.

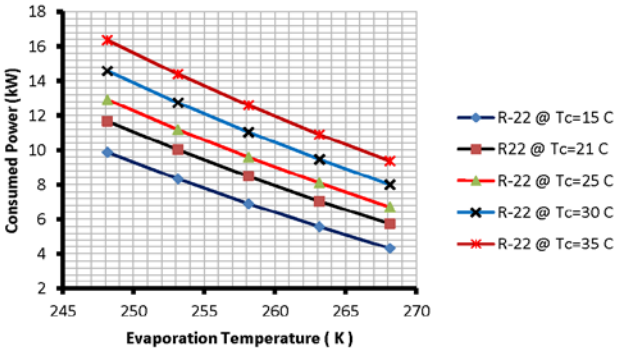

Figure 4. The variation of consumed power with evaporator and condensing temperatures

The results revealed that the power used by compressor exhibited an increase with condensing temperature which approaches a maximum of (16.3) kW at (-25) °C evaporator temperature and (35) °C condensing point. The trend of the data showed that the consumed power was the lowest at the lowest testing condensing temperature of (15) °C. The physical explanation for such behavior is that the discharge temperature and pressure out of the compressor are higher as the condensing temperature rises. This leads to an increase in the consumed power by the compressor. The coefficient of performance for R-22 system is shown in Figure 5. The data trend showed that (COP) of the chiller exhibited a deterioration with condensing temperature increase. This was due to the fact that increasing the condensing temperature requires higher power consumption for the same evaporation temperature, hence reducing the (COP) of the cooling unit. The higher (COP) corresponds to (8) was obtained at the lowest condensing value at evaporator temperature of (-5) °C. The lowest (COP) value corresponds to (2.1) estimated at (-25) °C evaporator temperature.

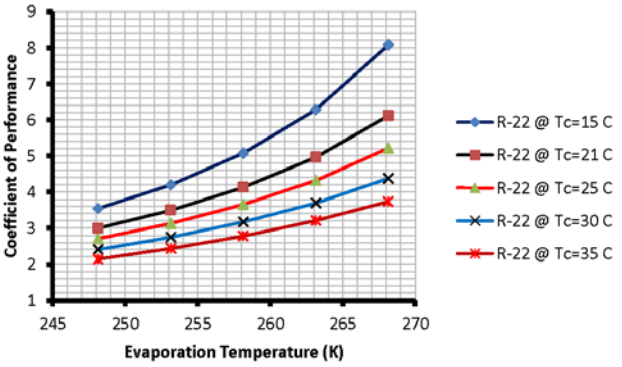

Figure 5. The variation of coefficient of performance of R-22 system with evaporator temperature.

The behavior of the (COP) with condensing temperature at various evaporator temperatures is illustrated in Figure 6. At constant evaporator temperature, the (COP) showed a nonlinear reduction variation with condensing temperature.

These curves are shifted uniformly as the evaporation temperature rises from the lowest values at (-25)°C approaching a maximum values at (-5) °C.

The condenser load required to accomplish the cooling load performed by the evaporator when circulating R-22 throughout the water chiller is shown in Figure 7.

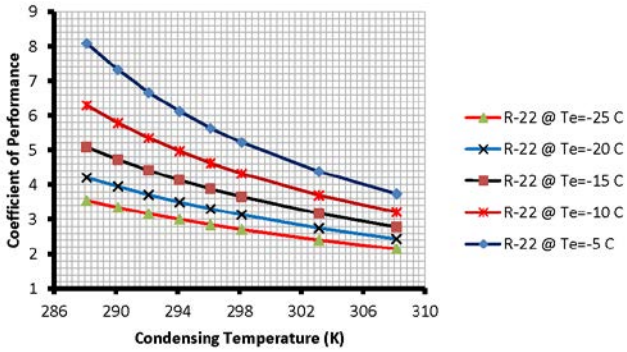

Figure 6. The variation of coefficient of performance of R-22 system with condensing temperature

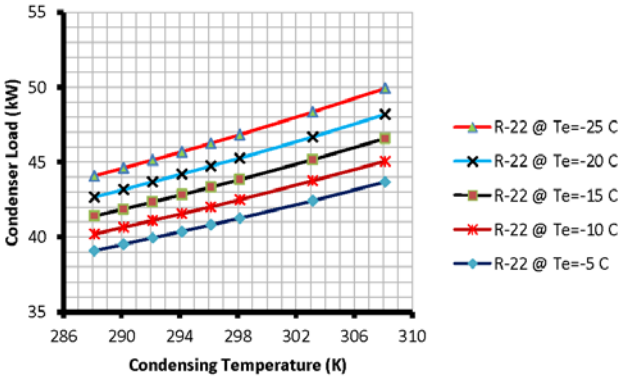

Figure 7. A comparison of condenser load variation with condensing temperature at various evaporator temperatures for R-22 system

The behavior of the predicted load reveals an increase of the condenser load with both of condensing temperature increase and evaporator temperature decrease. This phenomenon is mainly due to the increase of pressure lift through the compressor with condensing temperature increase or evaporation temperature decrease to attain the same high level temperature of condensation. Hence, the maximum condensing load was experienced at (-25) °C evaporator temperature to be (50) kW at (35) °C condensing temperature. This value is decreasing to approach a minimum at (-5) °C as (39) kW at (15) °C condensing point. The rest of tested condensing and evaporator temperature showed a range between those values of condensing loads.

3.2. Results Comparison

3.2.1. Coefficient of Performance

The (COP) of the investigated systems is compared at different evaporator temperatures as shown in Figure 8. All refrigerants showed the same data trend, the higher evaporator temperature operating condition reveals the higher (COP). Hence the maximum value of (COP) is experienced when circulating the test refrigerants at (-5) °C, Figure 8.a. It approaches a value of (8) and declines to about (3.6) at (15) °C and (35) °C respectively.

The lower evaporator test temperature (-25) °C exhibited the lowest (COP) of the water chiller unit. It declines from a peak value of about (4) to (2) at condensing temperatures of (15) °C and (35) °C respectively.

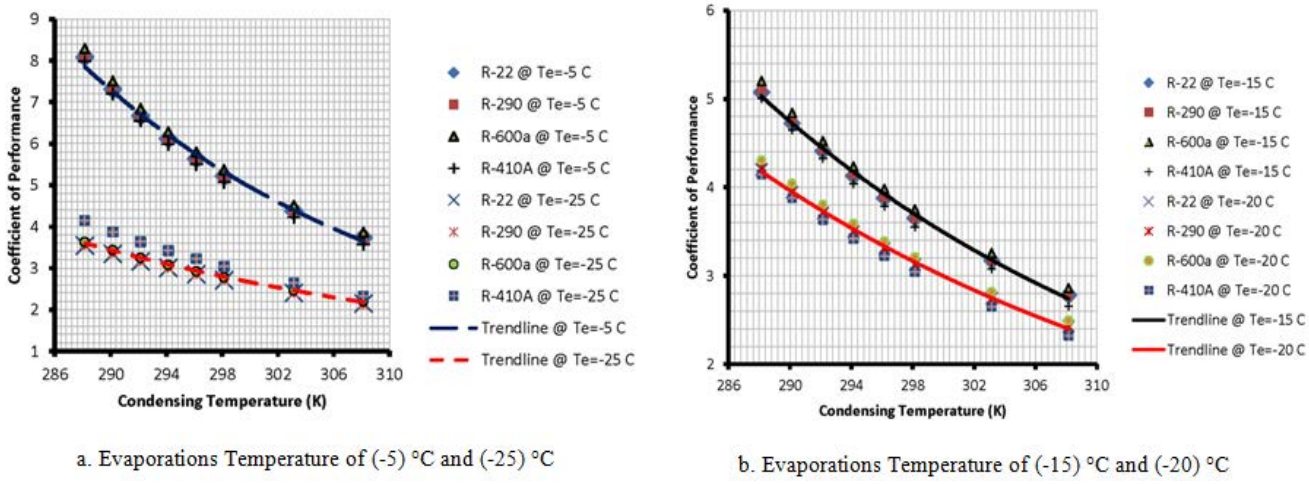

Figure 8. A comparison of (COP) variation with condensing temperature for test refrigerants

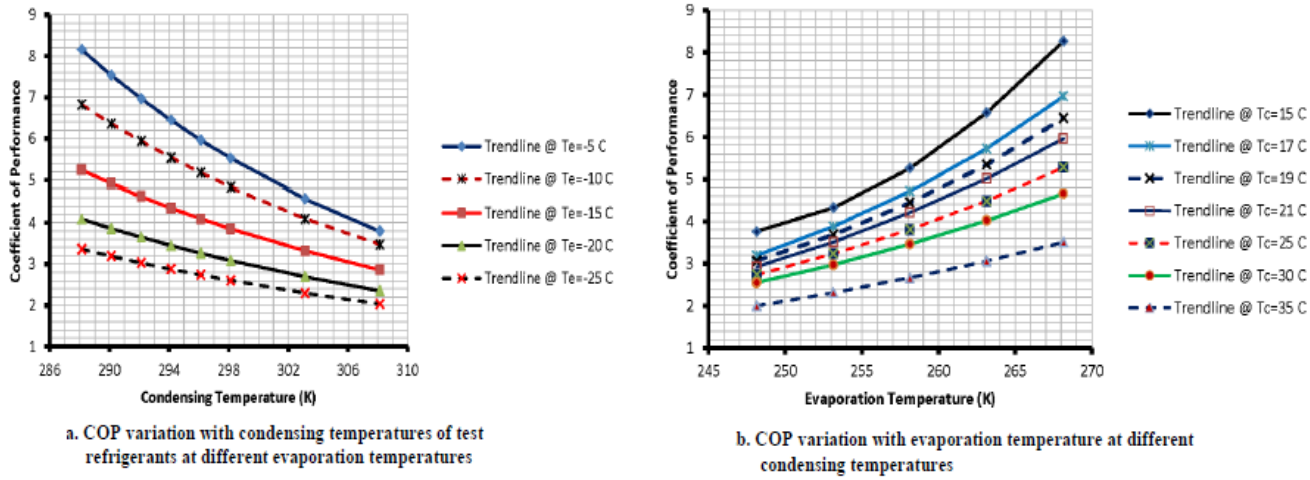

Figure 9. COP variation with evaporation and condensing temperatures of test refrigerants

The trend lines of the predicted data for all refrigerants showed similar characteristic behavior as illustrated in Figure 9. All curves showed that the maximum predicted values of (COP) are experienced at the lower condensing temperature and it reduces as the condensing temperature increases in a power fit relation.

Figure 9.b reveals that the highest condensing temperature of (35) °C showed the lowest (COP) regardless of the operating temperature of the evaporator and circulated refrigerant properties. Hence it is concluded that such operating condition for the condenser to be avoided as much as possible to prevent the deterioration of the chiller performance. Such operating conditions are usually controlled by the climate and altitude of the place where this equipment is utilized. R410A exhibited the lowest (COP) when compared with R-22; it was within the range of (1-5) % lower than that of R-22.

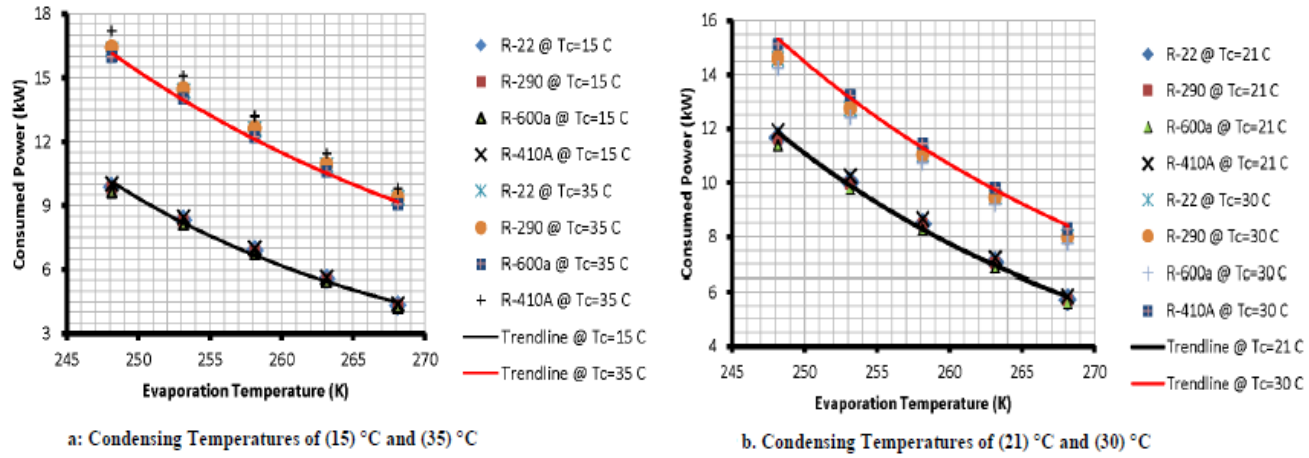

Figure 10. A comparison of chiller consumed power at different condensing temperatures for test refrigerants

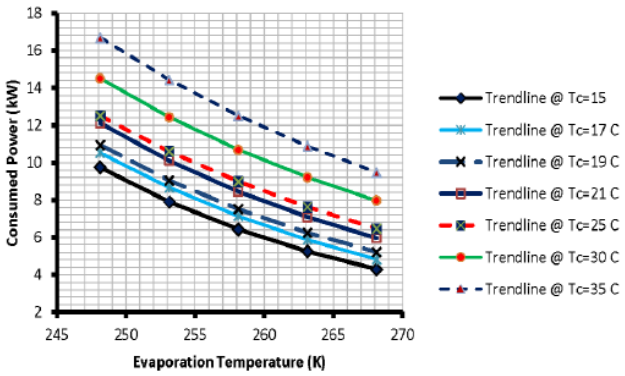

Figure 11. Consumed power variation with evaporation temperature at different condensing temperatures

3.2.2. Consumed Power

A comparison for the predicted consumed power by the compressor is shown in Figure 10 for four selected condensing temperatures. These charts show that the spent power to run the unit exhibited an increase with the condensing temperature increase and vice versa. They also reveal that the power consumed by R-290 is similar to that of the R-22 system. R-410A showed the highest power consumption among test refrigerants, it is in the range of (1-5) % higher than the corresponding values of R-22 for all of the investigated operating conditions. R-600a exhibited the lowest power consumption but was only within (3) % compared to that of the R-22 system.

The predicted maximum consumed power for R-410A was (17) kW registered at (-25) °C evaporator temperature and its lowest value was predicted at (-5) °C to be only (4) kW. The R-600a system needed about (16) kW at (35) °C condensing temperature. All refrigerants systems consumed nearly the same power at the highest test evaporator temperature of (-5) C. This explains why the predicted behavior of the power consumption is getting closer as the evaporation temperature increases for the same condensing temperature as shown Figure 9.

The data trend lines of the consumed power for all test refrigerants vary with the evaporator temperature in a similar pattern, Figure 11. Here, the trend of data behavior shows clearly that the consumed power increases with condensing temperature increase at constant evaporator temperature for all of the test range in this investigation.

3.2.3. Condenser Load

The comparison for the condenser load in the range of test operating conditions between the refrigerants is illustrated in Figure 12. The data are lied in the range of (39 to 51) kW for all of the test conditions. The lowest condenser load was experienced when circulating R-22 at (-5) °C and the highest was achieved when circulating R-410A at (35) °C.

Hence, R-410A refrigerant exhibited the highest load in comparison with R-22 among other circulated refrigerants by (1.5) %. R-600a showed a lower condenser load than that of the R-22 system by a negligible margin value to be within (0.5) %. The data trend lines for all test refrigerants exhibited a similar fashion, the condenser load showed a decrease with evaporator temperature increase and vice versa as shown in Figure 13. In general, the test operating conditions for these refrigerants revealed the same predicted data trending, the higher was achieved with the higher condensing temperature.

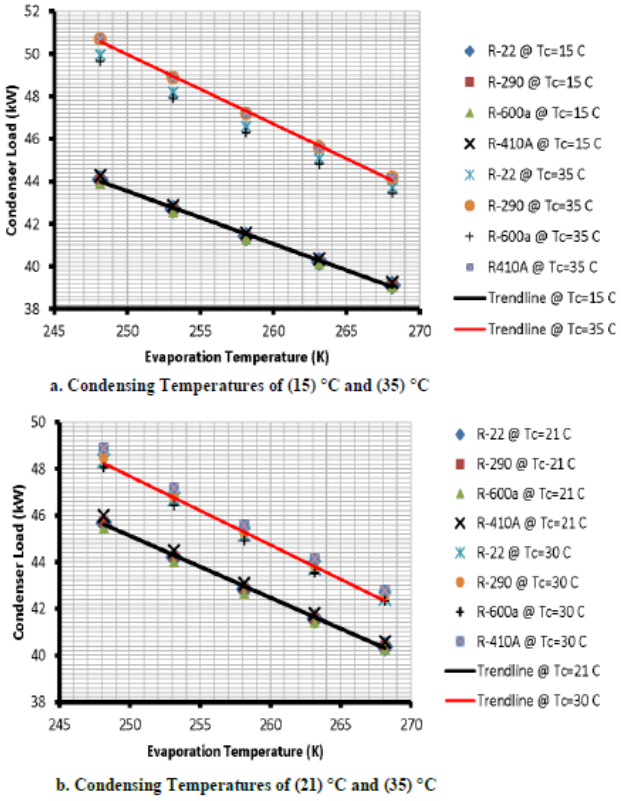

Figure 12. A comparison of chiller condenser load for test refrigerants

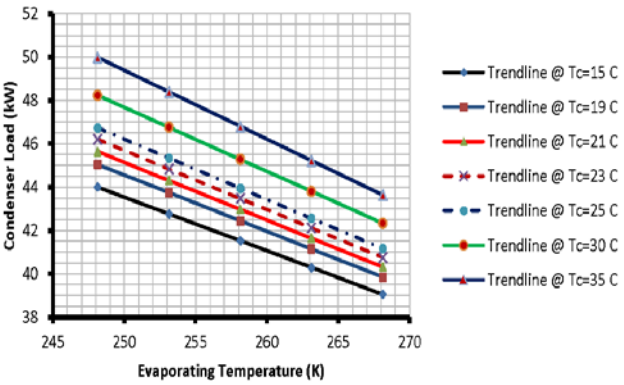

Figure 13. Condenser load variation with evaporation temperature at different condensing temperatures of test refrigerants

The behavior lines showed a linear variation for the condenser load with the evaporator temperature. Whereas, the consumed power of compressor and (COP) of the system showed a power fit relation with the evaporator temperature as shown in Figure 9 & Figure 11 above.

3.3. Underground Condenser Design

Although the design of the underground heat exchanger is out of the scope of this study but it is worthy to mention its sizing requirements. The flow of refrigerant through the condenser experience three different heat transfer modes. Namely, desuperheating zone followed by a condensation part and finally accomplishes the subcooling

of the liquid in the final zone, Figure 14. The thermal assessment of these zones is usually handled separately; the surface area of the condenser then is corresponding to the algebraic summation of area required by these zones.

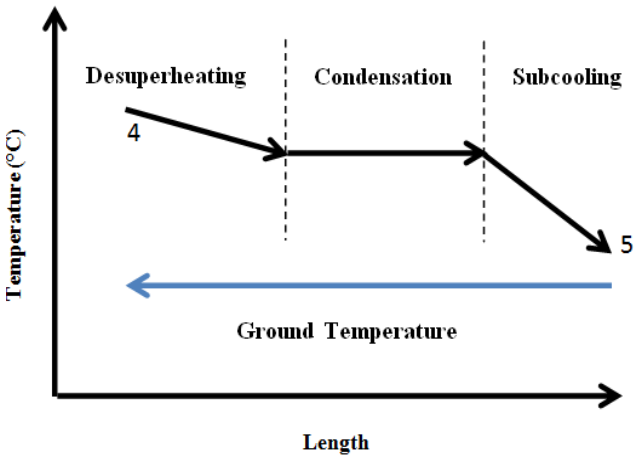

Figure 14. Heat transfer modes through the condenser

The heat transfer coefficient of the superheated gas corresponds to a quite low value compared to the subcooling heat transfer coefficient and condensation one. These two values are predicted from the available correlations of forced convection heat transfer. The phenomena of condensation and evaporation are well-studied for decades and numerous correlations are presented in the open literature to predict their heat transfer coefficients. The heat transfer coefficient for both heat transfer modes is quite high due to the change of phase experienced by the circulating fluid. The grout/soil properties control the heat transfer process, the thermal conductivity of the grout/soil represents the major factor which determines the overall heat transfer coefficient of the heat exchanger (U). Hence, it determines the underground heat exchanger size regardless of the refrigerant type.

$$\dot{Q}_{cond} = U\ A\Delta T_m. \tag{7}$$

The surface area required to reject the heat out of the condenser, then estimated from:

$$A = \frac{\dot{Q}_{cond}}{U\Delta T_m}. \tag{8}$$

The condensation temperature for pure fluids, non azeotrop mixtures, azeoptrop mixtures with negligible temperature glide takes place at constant temperature. Hence, for a constant ground temperature, the parameter ΔT_m could be estimated and the surface area of heat exchanger is assessed. Of course, the estimation of the surface area is not as simple as that since it is a time dependent and elaborated computational work is needed. Quite a good number of computer codes are commercially available to conduct the required calculations such as GLHEPRO V5.0 [19] and GLD [20].

4. Conclusions

The following conclusions could be inferred from this investigation:

1. Hydrocarbon refrigerants R-290 and R-600a and the azeotrop refrigerant R410A are suitable candidates to replace R-22 refrigerant with a low margin of discrepancy.
2. R-410A consumed more power to run the compressor and showed a lower (COP) than R-22 by the range of (1-5) % depending on the operating conditions presented here.
3. R-410A refrigerant exhibited the highest condenser load in comparison with R-22 among other circulated refrigerants by (1.5) %.
4. R-600a exhibited lower power consumption and revealed higher (COP) than that of R-22 by (3) % and showed almost similar condenser load as that of R-22 within (0.5) % deviation.
5. R-290 revealed similar performance as that of R-22 for power consumption, coefficient of performance and condenser load.
6. The general trend of the predicted performance of all refrigerants showed an increase in the compressor power consumption with condensing temperature increase, it approaches maximum at (35) °C.
7. All test refrigerants showed better performance when the evaporator temperature was fixed at (-5) °C. The data trend showed lower power consumption, lower condenser load and higher coefficient of performance.

Nomenclatures

A	Heat Exchanger Surface Area, (m^2)
COP	Coefficient of Performance of Refrigeration Unit
h	Fluid Enthalpy, (kJ/kg)
$\dot{m}$	Mass Flow Rate of Refrigerant, (kg/s)
$\dot{Q}$	Heat Transfer Rate, (kW)
ΔT	Temperature Difference, (°C)
U	Overall Heat Transfer Coefficient, (kW/m^2 K)
$\dot{W}$	Power Consumed, (kW)

Subscriptions

comp	Compressor
cond	Condenser
evap	Evaporator
is	Isentropic
m	Mean value
ref	Refrigerant
vol	Volumetric

Greek Letters

η	Compressor Efficiency (%)
ϕ	Any Predicted Performance Measure
ψ	Deviation Percentage (%)

Acknowledgements

The author would like to express his sincere thanks to the ACCUEIL SANS FRONTIERES 67 Association for their support to publish this work.

References

[1] Kim, D. H., Park, H. S. and Kim, M. S., "Characteristics of R134a/R410A Cascade Heat Pump and Optimization", International Refrigeration and Air Conditioning Conference at Purdue, Paper no. 2425, pp1-7, (2012).

[2] Kim, J., Lee, J. Choi, H, Lee S., Oh, S. and Park, W., Experimental study of R134a/R410A Cascade cycle for variable refrigerant flow heat pump systems, Journal of Mechanical Science and Technology, 29 (12), pp 5447-5458, 2015.

[3] Tarrad, A. H., "Thermodynamic Performance Evaluation for Low Temperature Heat Source Cascade System Circulating Environment Friendly Refrigerants," Int. J. Energy Environ. Sci., 2(2), pp. 36-47, March 2017.

[4] Tarrad, A. H., "Thermodynamic Analysis for Hybrid Low Temperature Sustainable Energy Sources in Cascade Heat Pump Technology," Asian J. Eng. Technol., 5(2), pp. 29-46, April 2017.

[5] Tarrad, A. H., "Performance Optimization for a Proper Heat Pump Technology Functions at Low Temperature Heat Source," Int. Res. J. Power Energy Eng., 2(1), pp. 19-34, June 2017.

[6] Tarrad, A. H., "Thermodynamic Evaluation for Intermediate Temperature Optimization in Low Temperature Heat Source Cascade Heat Pump Technology", Asian Journal of Engineering and Technology, Vol. 5 (5), pp. 126-139, October 2017.

[7] Tarrad, A. H., "Perspective Performance Evaluation Technique for a Cascade Heat Pump Plant Functions at Low Temperature Heat Source," Int. J. Econ. Energy Environ., 2(2), pp. 13-24, 2017.

[8] Tarrad, A. H., "A Perspective Evaluation Methodology for Economic Feasibility of Low Temperature Sustainable Energy Source in Heating Mode Technology", Transactions of the ASME, Journal of Energy Resources Technology, Vol. 140, pp. 020902-1 to 020902-10, February 2018.

[9] "Energy Efficiency and Renewable Energy", Guide to Geothermal Heat Pumps, U.S. Department of Energy, DOE/EE-0385, February 2011.

[10] Yrjölä, J. and Laaksonen, E., Domestic hot water production with ground source heat pump in apartment buildings, Energies, 8 (8), pp 8447-8466, 2015.

[11] Ali M H, Selamat S, Kariya K, Miyara A, "Experimental performance estimations of horizontal ground heat exchangers for GSHP system", 16th International Refrigeration and Air Conditioning Conference, Purdue, Paper 1808, Purdue University, USA, 2016.

[12] ASHRAE 34-2019, Designation and Safety Classification of Refrigerants, 2019.

[13] "Underground Propane Piping - Yard Line", Retrieved 25-08-2019. https://www.propane101.com/lpgasserviceline.htm.

[14] BS 4434: 1995 Specification for safety and environmental aspects in the design, construction and installation of refrigerating appliances and systems, BSI, London 1997.

[15] BS EN 378: 2000 Refrigerating systems and heat pumps – safety and environmental requirements, 2000.

[16] "Gases - Explosive and Flammability Concentration Limits". Retrieved 09-09-2013. https://www.engineeringtoolbox.com/explosive-concentration-limits-d_423.html.

[17] "Applications: Tube, Pipe & Fittings: Direct-Exchange Geothermal Heating/Cooling Technology". www.copper.org. Retrieved 11-17-2016.

[18] Technical University of Denmark (DTU), "CoolPack Software: A Collection of Simulation Tools for Refrigeration", Denmark. 2001.

[19] "Ground Loop Heat Exchanger Design Software", International Ground Source heat Pump Association (IGSHPA). https://hvac.okstate.edu/glhepro/overview.

[20] Gaia Geothermal. Ground Loop Design Software, GLD, 2009.